Canonical titration simulations

Amin Bakhshandeh[1] and Yan Levin[1, a)]
Instituto de Física, Universidade Federal do Rio Grande do Sul, Caixa Postal 15051, CEP 91501-970, Porto Alegre, RS, Brazil.

We present a Monte Carlo approach for performing titration simulations in the canonical ensemble. The standard constant pH (cpH) simulation methods are intrinsically grand canonical, allowing us to study the protonation state of molecules only as a function of pH *in the reservoir*. Due to the Donnan potential between a system and an (implicit) reservoir of a semi-grand canonical simulation, the pH of the reservoir can be significantly different from that of an isolated system, for an *identical* protonation state. The new titration method avoids this difficulty by using canonical reactive Monte Carlo algorithm to calculate the protonation state of macromolecules as a function of the total number of protons present inside the simulation cell. The pH of an equilibrated system is then calculated using a new surface insertion Widom algorithm, which bypasses the difficulties associated with the bulk Widom particle insertion for intermediate and high pH values. To properly treat the long range Coulomb force, we use Ewald summation method, showing the importance of the Bethe potential for calculating pH of canonical systems.

I. INTRODUCTION

The stability of colloidal particles in aqueous suspensions is intrinsically connected with their surface charge density, which is controlled by the pH of solution. Similarly the activity of many biologically relevant proteins and polyelectrolytes is controlled by solution's pH and ionic strength[1–18]. Quantitative understanding of charge regulation in such complex systems is, therefore, of a paramount importance in a wide range of industrial and medical applications. For some simple colloidal systems with a regular distribution of surface active groups, one can use the Poisson-Boltzmann theory with the charge regulation boundary condition to study the particle protonation state[19–32]. However, this approach breaks down for suspensions containing multivalent counterions or when dealing with flexible molecules, such as proteins or polyelectrolytes, whose three dimensional conformation is intimately coupled with the protonation state of the molecule. For such systems one is forced to rely on computer simulations[33–37].

pH is defined as the negative decadic logarithm of activity, $a_{\rm H} = c_{\rm H} e^{\beta \mu^{ex}_{\rm H}}$, of hydronium ions, $\mathrm{pH} = -\log_{10}(a_{\rm H}/c^{\ominus})$, where $c^{\ominus} = 1$ M is the standard reference concentration, $\beta = 1/k_B T$, and μ^{ex}_H is the excess electrochemical potential. The constant pH (cpH) Monte Carlo simulation method is a widely used approach for generating titration curves in systems undergoing protonation/deprotonation reactions[38]. However, an indiscriminate application of this method poses a fundamental problem. In cpH simulations, entities such as proteins, colloidal particles, or polyelectrolytes are confined within a simulation box, while protons and ions have the freedom to exchange with an acid and salt in an implicit external reservoir[34,35]. Consequently, the cpH simulation method is inherently semi-grand canonical. During the course of a cpH simulation, a proton is introduced into the system from an external reservoir held at a predetermined pH. To maintain charge neutrality within the simulation cell, one of the cations or protons within the bulk of the cell is arbitrarily removed. However, this arbitrary removal lacks adherence to the principle of detailed balance, potentially yielding inaccurate outcomes[39,40], except in cases where the system contains a substantial amount of salt and is highly diluted in polyelectrolyte/protein. Fortunately, it is easy to rectify the standard cpH algorithm[34,35] by incorporating a protonation step alongside a simultaneous grand canonical insertion of an anion. Conversely, a deprotonation step can be paired with a simultaneous grand canonical removal of an anion. This adjustment restores the detailed balance of the cpH algorithm, ensuring its internal consistency. We notice, however, that the simulation cell of such semi-grand canonical system will have a different mean electrostatic potential from that of the external reservoir. This is know as the Donnan potential. Therefore, the cpH simulation methods will allow us to predict the charge of polyelectrolyte only as a function of pH *in the reservoir*. Due to the presence of the Donnan potential, however, the pH of the reservoir, can be significantly different from that of an isolated system, for an identical protonation state[40,41]. Thus, if one compares the titration curves, in which, say, the charge of colloidal particles is plotted as a function of the pH of the reservoir, with the titration curves of an isolated (canonical) system, there can be very large difference between the two – in particular for large volume fraction suspensions of low ionic strength[40]. The difference between the two ensembles disappears in the limit or large ionic strength. This, perhaps, is the reason why this problem was not noticed previously – since most cpH simulations of proteins are performed at physiological concentrations and low protein volume fractions, when the difference between the two ensembles disappears. In fact, one can easily relate the pH_c of a canonical system, in which the number of ions and protons is the same as the averages obtained using a semi-grand canonical simulation with a reservoir

a)Electronic mail: levin@if.ufrgs.br

of pH_{gc}, using equation[40,41]

$$pH_c = pH_{gc} + \frac{\beta\varphi_D}{\ln(10)}, \tag{1}$$

where φ_D is the Donnan potential between the semi-grand canonical system and its external reservoir. We note, however, that the standard implementations of cpH simulations do not provide us with the value of the Donnan potential since it cancels out in the pair insertion/deletion moves used to preserve the charge neutrality during the simulation[34,35]. Recently, however, we have developed a new reactive grand canonical MC-Donnan (rGCMCD) method, which allows us to determine the Donnan potential directly within the simulation[40], allowing us to calculate both the titration isotherms of canonical and semi-grand canonical systems simultaneously – showing that for systems of low colloidal volume fraction and low ionic strength, the number of deprotonated groups can be 100% larger in an isolated system[40,41] compared to a system connected to a reservoir of exactly the same pH.

To perform rGCMCD simulations requires knowledge of the chemical potential of all ions present in the reservoir. This can be obtained using Widom's particle insertion method or by performing a separate grand canonical MC simulation just for the reservoir. There is also an additional complication that the Donnan potential must be calculated self-consistently during the simulation. Clearly, it is desirable to be able to obtain the titration curves directly for an isolated (canonical) system – without going through a semi-grand canonical algorithm. The difficulty is that in a canonical reactive MC simulation, one does not control the pH of the system, instead the total number of ions and protons present inside the simulation cell is specified. The simulation then determines how many of the protons will remain free and how many will be associated with the polyelectrolyte monomers. After the equilibrium is established, one can use Widom's particle insertion method[42,43] to calculate the excess chemical potential of protons:

$$\mu^{ex} = -k_B T \ln\left(\langle \exp(-\beta\Delta E)\rangle_0\right), \tag{2}$$

where ΔE is the energy difference between a system with a virtual proton and without. The subscript 0 on the brackets indicates that the sampling for calculating the average is performed using the unperturbed system, without the virtual proton. To obtain pH, however, one also needs the average concentration of free hydronium ions inside the cell. For intermediate and large pH, however, there might not be any free hydroniums present inside the simulation cell at all, preventing us from accurately calculating the pH of the system. To overcome this difficulty, in this paper we will introduce a new surface Widom insertion algorithm to easily and accurately calculate the pH of a canonical system undergoing protonation/deprotonation reactions.

The paper is organized as follows: In section II we briefly review the canonical reactive MC algorithm[36,37,39], in section III we preset a new surface Widom insertion method and discuss the modification of the usual Ewald summation necessary to properly account for the electrostatics of an infinite charge non-neutral system. We will also compare the titration isotherms calculated using the canonical simulation algorithms with the ones obtained using rGCMCD method. Finally, the discussion and conclusions will be presented in the section IV.

II. REACTIVE CANONICAL METHOD

Consider a polyelectrolyte or a colloidal particle with monomers that can undergo a protonation deprotonation reaction:

$$HA \rightleftarrows H^+ + A^- \tag{3}$$

with acid dissociation constant constant K_a.

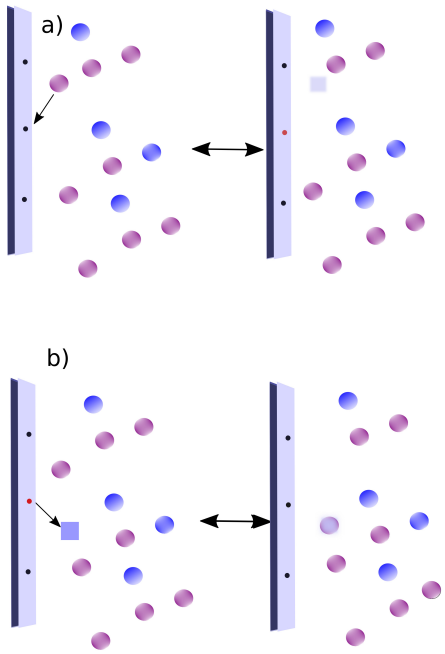

FIG. 1: The canonical reactive MC moves. Left panels show "old" and right panel "new" configuration: a) shows a protonation move – a proton from bulk adsorbs to the site. b) shows a deprotonation move, proton desorbs from the surface and forms a hydronium in the bulk. The red spheres are hydronium ions and blue spheres are coins. Salt ions are not shown.

In a canonical reactive MC simulation there are two types of movements: the bulk movements in which positions of ions are randomly changed with the acceptance probabilities given by the usual Metropolis algorithm; and reaction protonation/deprotonation moves, see Fig. 1. To construct a MC algorithm for the reaction moves, we first observe that the acid dissociation constant is the

inverse of the two body partition function for the formations of a HA molecule. Thus, when a proton is transferred from the bulk to the surface, where it will react with a surface group A^-, there are two changes that occur in the system: change of electrostatic energy ΔE and change in the chemical energy $k_BT\ln(K_a/c^{\ominus})$. The probabilities for the old (o) and new (n) configurations during a protonation move are proportional to:

$$\Pi_o \sim \frac{V^{N_H}}{N_H!}e^{-\beta E_{N_H}},$$
$$\Pi_n \sim \frac{V^{N_H-1}}{(N_H-1)!}e^{-\beta E_{N_H-1}-\ln\frac{K_a}{c^{\ominus}}}, \quad (4)$$

where N_H is the number of free hydronium ions inside the simulation cell, and V is the volume of the cell. For a deprotonation move, we have

$$\Pi_o \sim \frac{V^{N_H}}{N_H!}e^{-\beta E_{N_H}},$$
$$\Pi_n \sim \frac{V^{N_H+1}}{(N_H+1)!}e^{-\beta E_{N_H+1}+\ln\frac{K_a}{c^{\ominus}}}. \quad (5)$$

Using the usual detailed balance argument, the acceptance probabilities for the deprotonation and protonation moves can now be written as:

$$P_d = \min\left[1, \frac{VK_a}{N_H+1}e^{-\beta\Delta E}\right],$$
$$P_p = \min\left[1, \frac{N_H}{VK_a}e^{-\beta\Delta E}\right]. \quad (6)$$

If during the deprotonation move the new coordinate falls into the interior of a colloidal particle, the ΔE is counted as infinite, and the move is rejected. The change in electrostatic energy during each move is calculated using Ewald summation with tin foil boundary condition. The Coulomb energy of a periodically replicated charged system is:

$$E = \frac{1}{2}\sum_{ij}{}'\sum_{\boldsymbol{n}}\frac{q_iq_j\mathrm{erfc}(\kappa_e|\boldsymbol{r}_i-\boldsymbol{r}_j-L\boldsymbol{n}|)}{\epsilon_w|\boldsymbol{r}_i-\boldsymbol{r}_j-L\boldsymbol{n}|}$$
$$+\sum_{k\neq 0}\frac{2\pi\exp(-\boldsymbol{k}^2/4\kappa_e)}{\epsilon_w V\boldsymbol{k}^2}(A(\boldsymbol{k})^2+B(\boldsymbol{k})^2)$$
$$-\sum_i\frac{q_i^2\kappa_e}{\epsilon_w\sqrt{\pi}}, \quad (7)$$

where

$$A(\boldsymbol{k}) = \sum_i q_i\cos(\boldsymbol{k}\cdot\boldsymbol{r}_i), \quad (8)$$
$$B(\boldsymbol{k}) = \sum_i q_i\sin(\boldsymbol{k}\cdot\boldsymbol{r}_i),$$

$\boldsymbol{n} = (n_1, n_2, n_3)$ are integers, and $\boldsymbol{k} = (\frac{2\pi}{L}n_1, \frac{2\pi}{L}n_2, \frac{2\pi}{L}n_3)$ are the reciprocal lattice vectors for the cubic simulation box of side length L and volume $V = L^3$. The prime on the sum indicates that $i = j$ term is excluded from the summation when $\mathbf{n} = 0$. The electrostatic energy is invariant with respect to the damping parameter κ_e, which we set to $\kappa_e = 5/L$, where L is the side length of the cubic simulation cell. With this choice of κ_e, the sum over $\mathbf{n}$ can be replaced by the simple periodic boundary condition for the short range (erfc term) contribution to the electrostatic energy.

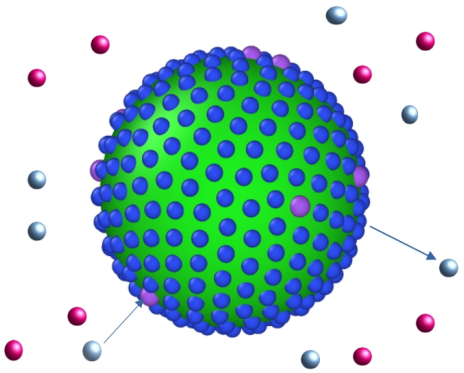

FIG. 2: A colloidal particle inside the simulation cell. The blue sites are protonated. The gray spheres are the hydronium ions. The arrows indicate protonation/deprotonation moves.

III. SURFACE WIDOM METHOD

To perform the simulations we use a cubic simulation box of side length L that contains either colloidal particles, polyelectrolyte, or protein molecules in a completely deprotonated state. In the present discussion we will use a primitive model, which treats water as a uniform dielectric continuum of Bjerrum length $\lambda_B = q^2/k_BT\epsilon_w = 7.2$ Å, where q is the proton charge and ϵ_w is the dielectric constant of water. There is, however, no difficulty to modify the algorithm to account for the explicit water or to combine it with a molecular dynamics simulation. The simulation cell also contains fully dissociated salt and acid ions — H_3O^+, Cl^-, and Na^+. We start the simulation with the number of H_3O^+ equal to the number of negatively charged polyelectrolyte monomers. We then run the reactive canonical MC algorithm described above to obtain the equilibrium number of protonated groups and the number of free hydronium ions, see Fig. 2 . Note that in a canonical simulation we do not have a direct access to the pH, which will be determined by the activity of hydronium ions in equilibrium. This can only be obtained using a separate Widom like particle insertion simulation that will allow us to probe the electrochemical potential of hydronium ions after the equilibrium has been established. To change pH inside the system, we can add a base such as NaOH. Since the spontaneous hydrolysis of water is so weak, addition of 1 base molecule will result in the formation of one water

molecule, and an appearance of a Na^+ ion inside the simulation box. The net effect is, therefore, a replacement $1H^+ \rightarrow 1Na^+$. We can then rerun the simulation to obtain the new protonation state. Repeating this process until all hydroniums are replaced by Na^+, we can cover the full pH range.

The crucial part of a canonical titration MC is the calculation of pH after the system has equilibrated. The standard Widom particle insertion method is usually not very practical, since to calculate the pH we need the whole electrochemical potential inside the simulation cell, and not just its excess part. At moderate to high pH, the interior of the simulation cell might not have any free hydronium ions at all, preventing us from accurately calculating the electrochemical potential and the activity of hydronium ions. On the other hand, since the condensed protons are in equilibrium with the hydronium ions in the bulk and, therefore, have exactly the same electrochemical potential, we can use them to accurate calculate the pH inside the system. There is, however, an additional complication when working with infinitely replicated Coulomb systems. The Ewald summation, effectively leads to a macroscopic crystal composed of replicated microscopic simulation cells. In general, a simulation cell will have a net electric dipole moment $\boldsymbol{M} = \sum_i q_i \boldsymbol{r}_i$ and a finite second moment of the charge density tensor. From the electrostatics it is well known that such uniform polarization is analogous to the surface charge density $\boldsymbol{M} \cdot \boldsymbol{n}/V$, where $\boldsymbol{n}$ represents the unit normal to the boundary of the macroscopic spherical crystal, see Fig. 3. This effective surface charge, will lead to electric field in the interior of the crystal. Similarly the fact that in general the simulation cell has a non-zero moment of the charge density tensor, results in a dipolar layer at the surface of the macroscopic crystal[44] – so that interior of the crystal has different mean electrostatic potential compared to the exterior[40]. This potential difference is known as the Bethe potential and for a charge neutral systems is given by:

$$\phi_B = -\frac{2\pi}{3\epsilon_w V} \sum_i q_i {\boldsymbol{r}_i}^2. \tag{9}$$

The derivation of this results within Ewald formalism is provided in the Appendix A. When the macroscopic crystal is "wrapped" in a tin foil, the induced image charge will kill off the surface contribution to the electrostatic potential. In general, it is known that for liquid state systems, calculations based on Ewald summation with tin foil boundary condition tend to be more accurate than the ones based on "vacuum" boundary conditions. However, in order to implement the Widom particle insertion method the system must be "unwrapped" from the tin foil, so that a proton can be brought from outside into the simulation cell. As the proton enters the crystal it will experience a jump in the electrostatic potential given by $q\phi_B$. Note, that the Bethe potential is not constant – it depends on the instantaneous positions of all the charges inside the simulation cells.

To make the discussion more concrete, consider a colloidal particle with Z active surface groups placed at the center of a cubic simulation cell, see Fig. 2. The cell also contains some number of H_3O^+, Cl^-, and Na^+ ions and is overall charge neutral. We now run the reactive MC simulation to calculate how many of Z surface groups will become protonated. After the system has relaxed to equilibrium, we find that on average N of the surface sites are protonated. The canonical partition function of a colloidal particle with N protonated sites can be written as:

$$Q(N) = \frac{1}{N!} \operatorname{Tr}\left[\mathrm{e}^{-\beta(E_N + N k_b T \ln(\frac{\mathrm{K}_a}{c^\ominus})}\right], \tag{10}$$

where the Tr refers to the trace over all the microstates of *both* ions and protons inside the system. The electrochemical potential of a proton is the difference in free energy of two systems: one in which the colloidal particle has N protonated sites and the other $N+1$ protonated sites,

$$\beta\mu_{\mathrm{H}} = -\ln \frac{Q(N+1)}{Q(N)}. \tag{11}$$

We can rewrite this as

$$\mathrm{e}^{-\beta\mu_H} = \frac{c^\ominus Z}{K_a\,(N+1)} \left\langle \mathrm{e}^{-\beta(\Delta E + q\phi_B)} \right\rangle_0, \tag{12}$$

where ΔE is the difference in electrostatic energy between systems with N and $N+1$ protonated groups, and ϕ_B is the Bethe potential that the virtual proton gains after entering into the Ewald "crystal". Since Ewald sum periodically replicates the whole simulation cell, it will also replicate the virtual proton. A periodic charge non-neutral system will have an infinite energy. To avoid this, together with the virtual proton, in the calculation of E, we also introduce a uniform neutralizing background, which regularizes the electrostatic energy calculation, see Appendix A. The average in Eqn. (12) is calculated using the ensemble average of the unperturbed (without virtual proton) system. We notice that the left hand side of Eqn. (12) is $c^\ominus/a_{\mathrm{H}^+}$. Taking the decadic logarithm of the two sides of this equation, we finally obtain

$$\begin{aligned} \mathrm{pH} = &-\log_{10}\left(\frac{N+1}{Z}\right) + \mathrm{pK}_a + \\ &\log_{10}\left(\left\langle \mathrm{e}^{-\beta(\Delta E + q\phi_B)} \right\rangle_0\right), \end{aligned} \tag{13}$$

where the subscript 0 on $\langle ... \rangle_0$ indicates that the sampling for the averages and the system evolution between the virtual proton insertion events are performed using the energy of the unperturbed system.

The surface Widom insertion method brings a virtual proton from infinity into contact with a randomly selected colloidal active site; if the site is empty (has charge $-q$), it "reacts" with the virtual proton and its charge changes to 0 and the difference in electrostatic energy

between the protonated state and the original deprotonated state, ΔE, is calculated using Eqn. (A9). The average in Eqn. (13) is obtained using 5,000 uncorrelated insertion events. If the site is already protonated, the virtual proton will overlap with the real proton, resulting in infinite ΔE. The virtual protonation process does not affect the actual state of the site and is used just to probe the chemical potential.

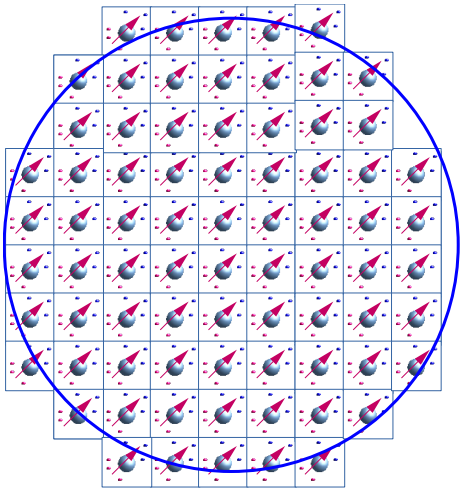

FIG. 3: Spherically replicated simulation cell, forming a macroscopic crystal. Each cell has a net electric dipole moment and a non-zero second moment of the charge density tensor. This results in a dipole layer and surface charge at the crystal boundary, producing an electrostatic potential in the crystal's interior.

To validate the new approach, we used it to calculate the titration isotherms of 11% volume fraction suspension of nanoparticles of radius 60 Å with $Z = 600$ surface sites. For simplicity, we placed only one nanoparticle into the simulation cell, however, there is no conceptual difficulty in putting as many particles as is desired into the simulation cell. The simulation was performed inside a cubic cell, which in addition to the nanoparticle also contained 600 hydronium ions and four Na^+ and Cl^- ions, corresponding to the concentration of 1mM of salt. To calculate the titration isotherm, we ran the reactive MC simulation with the acceptance probabilities for protonation/deprotonation moves given by Eq. (6). After equilibration, the number of protonated sites was determined. To make sure the system was well equilibrated, we used 1 million particle moves. To check equilibrium we also monitored the energy of the system. After equilibration, we performed insertions of a virtual proton to calculate the pH using the surface Widom insertion method, Eq. (13). Virtual insertions were performed at interval of 10,000 particle moves, to make sure the events were uncorrelated. We then replaced one of the initial 600 hydroniums by Na^+ and repeated the calculation – resulting in a slightly more negatively charged nanoparticle and a slightly higher pH. We repeated this procedure until almost all the hydronium ions were replaced by Na^+, resulting in a nanoparticle with no protonated surface groups. We can summarize the sequence of calculations as follows:

1. Randomly distribute fully deprotonated colloidal particles, protons, and other ions inside the simulation cell.
2. Perform canonical moves and protonation/deprotonation moves using Eq. (6) to reach the equilibrium.
3. Attempt a surface protonation by a virtual proton.
4. Calculate the energy difference between protonated and deprotonated states and record the value of $e^{-\beta(\Delta E + q\phi_B)}$.
5. Perform 10^4 canonical and protonation/deprotonation particle moves to fully discorrelate the system.
6. Repeat step 2
7. After 5000 virtual proton insertion attempts, calculate $\left\langle e^{-\beta(\Delta E + q\phi_B)} \right\rangle_0$ and pH using Eq. (13).
8. Randomly replace one of the protons by Na^+ and go to step 5. It is possible to replace more than one protons by sodium ions, depending on how smooth the titration curve is desired.
9. When there are no protons left in the system, the simulation stops.

The titration isotherm calculated using this procedure is presented in Fig. 4. As a benchmark to check the accuracy of the new canonical titration method, we compared our results with the ones calculated using rGCMCD simulation[40]. We see a perfect agreement between the two methods. We have then repeated the calculation for a system with 50mM of salt. Again the agreement between the two simulation methods is excellent, see Fig. 5

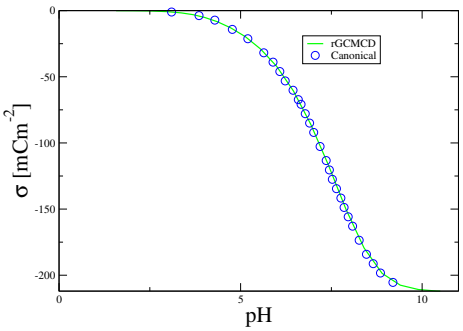

FIG. 4: Canonical titration of a suspension of 11% volume fraction (circles), containing nanoparticles of radius 60 Å with $Z = 600$ surface groups and 1 mM salt. The solid green curve is the benchmark calculated using rGCMCD simulation method of ref.[40].

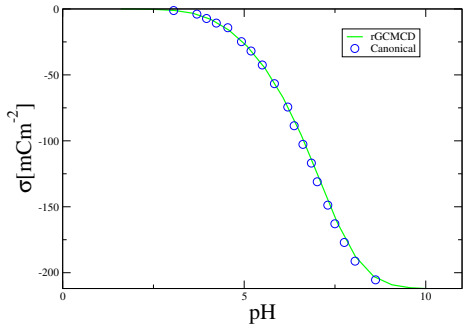

FIG. 5: Canonical titration of a suspension of 11% volume fraction (circles) containing nanoparticles of radius 60 Å with $Z = 600$ surface groups and 50 mM salt. The solid green curve is the benchmark calculated using rGCMCD simulation method of ref.[40].

IV. CONCLUSIONS

We have introduced a new Monte Carlo approach to calculate the titration isotherms in a canonical ensemble. Unlike conventional constant pH (cpH) simulation methods, which inherently operate in the grand canonical ensemble and assess the protonation state of molecules solely with respect to the pH within the reservoir, our canonical titration method works directly with the isolated system. The simulation method employs a reactive Monte Carlo algorithm to determine the protonation state of macromolecules in relation to the total number of protons present within the canonical simulation cell. To compute the pH of a fully equilibrated system, we have developed a new surface insertion Widom algorithm, which effectively circumvents the challenges associated with the bulk Widom particle insertion, particularly for extremely low hydronium ion concentrations. To accurately account for the long-range Coulomb forces, we have adopted the Ewald summation method, highlighting the significance of the Bethe potential in the precise calculations of pH of canonical systems. Although the present simulation method was developed within the framework of the primitive model, in which water is treated as a dielectric continuum, there is no conceptual difficulty of extending it to more realistic atomistic simulations. In this respect, the canonical approach is much easier to implement than the alternative grand canonical methods, which require a simultaneous insertion of an anion together with a protonation move, in order to preserve the overall charge neutrality[40]. Clearly in a dense system with atomistic water, most of insertion attempts will be rejected. On the other hand, one can easily combine the present canonical approach with a molecular dynamics (MD) simulation – so that the evolution of the system is performed using standard MD algorithms with a suitable thermostat – combined with titration moves in which one of the hydronium ions is transformed into a water molecule, with a proton transferred to one of the polyelectrolyte sites. The acceptance probability for such a protonation move will be given by Eq. (6), and similarly for a deprotonation move. The pH calculation introduced in this paper can also be combined with standard MD algorithms, so that the sampling needed to perform the average in Eq. (13) can be performed using a MD simulation. The implementation of the present approach to atomistic system will be the subject of the future work.

V. ACKNOWLEDGMENTS

This work was partially supported by the CNPq, the CAPES, and the National Institute of Science and Technology Complex Fluids INCT-FCx.

Appendix A: Electrostatic potential

Here, we briefly review the derivation of the electrostatic potential and energy in a periodically replicated system of cubic cells, with an excess charge $Q_t = \sum_i \mathrm{q}_i$, requiring presence of a uniform neutralizing background[40]. The electrostatic potential within the simulation cell is:

$$\begin{aligned}\phi(\boldsymbol{r}) \;=\; & \sum_{\boldsymbol{k}=\boldsymbol{0}}^{\infty}\sum_{j=1}^{N}\frac{4\pi \mathrm{q}_j}{\epsilon_w V|\boldsymbol{k}|^2}\exp\left[-\frac{|\boldsymbol{k}|^2}{4\kappa_e^2}+i\boldsymbol{k}\cdot(\boldsymbol{r}-\boldsymbol{r}_j)\right]+\\ & \sum_{j=1}^{N}\sum_{\boldsymbol{n}}\mathrm{q}_j\frac{\mathrm{erfc}(\kappa_e|\boldsymbol{r}-\boldsymbol{r}_j-L\boldsymbol{n}|)}{\epsilon_w|\boldsymbol{r}-\boldsymbol{r}_j-L\boldsymbol{n}|}\\ & +\frac{1}{V}\sum_{\boldsymbol{k}=\boldsymbol{0}}^{\infty}\tilde{\phi}_b(\boldsymbol{k})\exp[i\boldsymbol{k}\cdot\boldsymbol{r}]\;, \end{aligned} \tag{A1}$$

where

$$\tilde{\phi}_b(\boldsymbol{k}) = -\frac{4\pi Q_t}{\epsilon_w V}\frac{\int_V \mathrm{e}^{-i\boldsymbol{k}.\boldsymbol{r}}d^3r}{k^2}, \tag{A2}$$

is the Fourier transform of the background potential. The singular part of the background potential is $\phi_{b,s}$ as $\tilde{\phi}_b(\boldsymbol{k}) \equiv \tilde{\phi}_{b,s}\delta_{\boldsymbol{k0}}$, where we have defined the Kronecker delta for the zero mode, $\delta_{\boldsymbol{k0}}$. Performing the limit $\boldsymbol{k}\to 0$, we obtain[40]

$$\tilde{\phi}_{b,s} = -\frac{4\pi Q_t}{\epsilon_w k^2}+\frac{\pi Q_t L^2}{6\epsilon_w}. \tag{A3}$$

If one expands the first term of Eq. A1 around $\boldsymbol{k}=0$. The singular terms are:

$$\begin{aligned}& \frac{4\pi}{V\epsilon_w k^2}\sum_{j=1}\mathrm{q}_j-\frac{\pi}{\epsilon_w V\kappa_e^2}\sum_{j=1}\mathrm{q}_j+\\ & \frac{4\pi}{V\epsilon_w}\sum_{j=1}\mathrm{q}_j\frac{i\boldsymbol{k}\cdot(\boldsymbol{r}-\boldsymbol{r}_j)}{|\boldsymbol{k}|^2}-\\ & \frac{2\pi}{V\epsilon_w}\sum_{j=1}\mathrm{q}^j\frac{[\boldsymbol{k}\cdot(\boldsymbol{r}-\boldsymbol{r}_j)]^2}{|\boldsymbol{k}|^2}\;, \end{aligned} \tag{A4}$$

which can be shown[40] to lead to electrostatic potential within the simulation cell:

$$\varphi(\boldsymbol{r}) = \sum_{\boldsymbol{k}\neq 0}^{\infty}\sum_{j=1}^{N}\frac{4\pi \mathrm{q}_j}{\epsilon_w V|\boldsymbol{k}|^2}\exp\left[-\frac{|\boldsymbol{k}|^2}{4\kappa_e^2}+i\boldsymbol{k}\cdot(\boldsymbol{r}-\boldsymbol{r}_j)\right]$$
$$+\sum_{j=1}^{N}\sum_{\boldsymbol{n}}\mathrm{q}_j\frac{\mathrm{erfc}(\kappa_e|\boldsymbol{r}-\boldsymbol{r}_j-L\boldsymbol{n}|)}{\epsilon_w|\boldsymbol{r}-\boldsymbol{r}_j-L\boldsymbol{n}|} \quad \text{(A5)}$$
$$-\frac{\pi Q_t}{\epsilon_w V\kappa_e^2}+\frac{4\pi}{3\epsilon_w V}\boldsymbol{r}\cdot\boldsymbol{M}+\phi_B, \quad \text{(A6)}$$

where the Bethe potential is

$$\phi_B = -\frac{2\pi}{3\epsilon_w V}\sum_i \mathrm{q}_i\boldsymbol{r}_i^2+\frac{\pi Q_t}{6\epsilon_w L}. \quad \text{(A7)}$$

The electrostatic energy can be calculate from

$$E = \frac{1}{2}\int \rho_q(\boldsymbol{r})\varphi(\boldsymbol{r})d^3\boldsymbol{r}$$
$$= \frac{1}{2}\sum_i q_i\lim_{\boldsymbol{r}\to\boldsymbol{r}_i}\left[\varphi(\boldsymbol{r})-\frac{q_i}{\epsilon_w|\boldsymbol{r}-\boldsymbol{r}_i|}\right]-$$
$$\frac{Q_t}{2V}\lim_{\boldsymbol{k}\to\boldsymbol{0}}\tilde{\varphi}(\boldsymbol{k}), \quad \text{(A8)}$$

which leads to [40]

$$E = \frac{1}{2}{\sum_{ij}}'\sum_{\boldsymbol{n}}\frac{q_iq_j\mathrm{erfc}(\kappa_e|\boldsymbol{r}_i-\boldsymbol{r}_j-L\boldsymbol{n}|)}{\epsilon_w|\boldsymbol{r}_i-\boldsymbol{r}_j-L\boldsymbol{n}|}$$
$$+\sum_{k\neq 0}\frac{2\pi\exp(-\boldsymbol{k}^2/4\kappa_e)}{\epsilon_w V\boldsymbol{k}^2}(A(\boldsymbol{k})^2+B(\boldsymbol{k})^2)$$
$$-\sum_i\frac{q_i^2\kappa_e}{\epsilon_w\sqrt{\pi}}-\frac{\pi Q_t^2}{2\epsilon_w V\kappa_e^2}+\frac{2\pi}{3\epsilon_w V}\boldsymbol{M}^2. \quad \text{(A9)}$$

In our simulations, the periodically replicated system has tin-foil boundary condition, so that the $\boldsymbol{M}$ dependent contribution to the total energy vanishes. For neutral systems $Q_t = 0$.

[1] H.-J. Butt, *Journal of Colloid and Interface Science*, 1994, **166**, 109–117.
[2] Y. Levin, *Reports on progress in physics*, 2002, **65**, 1577.
[3] D. Andelman, *Soft condensed matter physics in molecular and cell biology*, 2006, **6**, year.
[4] M. Borkovec, B. Jönsson and G. J. M. Koper, in *Ionization Processes and Proton Binding in Polyprotic Systems: Small Molecules, Proteins, Interfaces, and Polyelectrolytes*, ed. E. Matijević, Springer US, Boston, MA, 2001, pp. 99–339.
[5] J. N. Israelachvili, *Intermolecular and surface forces*, Academic press, 2011.
[6] D. C. Grahame, *Chemical reviews*, 1947, **41**, 441–501.
[7] L. Guldbrand, B. Jönsson, H. Wennerström and P. Linse, *The Journal of chemical physics*, 1984, **80**, 2221–2228.
[8] J. López-García, M. Aranda-Rascón and J. Horno, *Journal of Colloid and Interface Science*, 2007, **316**, 196–201.
[9] R. O. James and G. A. Parks, in *Surface and colloid science*, Springer, 1982, pp. 119–216.
[10] P. Attard, *Current Opinion in Colloid & Interface Science*, 2001, **6**, 366–371.
[11] S. L. Carnie, D. Y. Chan and J. S. Gunning, *Langmuir*, 1994, **10**, 2993–3009.
[12] M. Hermansson, *Colloids and surfaces B: Biointerfaces*, 1999, **14**, 105–119.
[13] B. W. Ninham, *Advances in colloid and interface science*, 1999, **83**, 1–17.
[14] E. J. W. Verwey, *The Journal of Physical and Colloid Chemistry*, 1947, **51**, 631–636.
[15] A. Bakhshandeh, *Chemical Physics*, 2018, **513**, 195–200.
[16] R. Lunkad, F. L. Barroso da Silva and P. Košovan, *Journal of the American Chemical Society*, 2022, **144**, 1813–1825.
[17] S. Zhou, *Molecular Physics*, 2023, e2216632.
[18] S. Zhou, *Molecular Physics*, 2022, **120**, e2094296.
[19] K. Linderstrøm-Lang, *Comptes Rendus des Travaux du Laboratorie Carlsberg*, 1924, **15**, 1–29.
[20] B. W. Ninham and V. A. Parsegian, *J. Theor. Biol.*, 1971, **31**, 405–428.
[21] D. Frydel, *J. Chem. Phys.*, 2019, **150**, 194901.
[22] R. Podgornik, *The Journal of Chemical Physics*, 2018, **149**, 104701.
[23] Y. Avni, D. Andelman and R. Podgornik, *Current Opinion in Electrochemistry*, 2019, **13**, 70–77.
[24] T. Markovich, D. Andelman and R. Podgornik, *EPL (Europhysics Letters)*, 2016, **113**, 26004.
[25] G. M. Ong, A. Gallegos and J. Wu, *Langmuir*, 2020, **36**, 11918–11928.
[26] A. Bakhshandeh, D. Frydel and Y. Levin, *Phys. Chem. Chem. Phys.*, 2020, **22**, 24712–24728.
[27] A. Bakhshandeh, D. Frydel, A. Diehl and Y. Levin, *Phys. Rev. Lett.*, 2019, **123**, 208004.
[28] A. Bakhshandeh, M. Segala and T. Escobar Colla, *Macromolecules*, 2022, **55**, 35–48.
[29] A. Bakhshandeh, D. Frydel and Y. Levin, *Langmuir*, 2022, **38**, 13963–13971.
[30] T. Curk and E. Luijten, *Phys. Rev. Lett.*, 2021, **126**, 138003.
[31] T. Curk, J. Yuan and E. Luijten, *The Journal of Chemical Physics*, 2022, **156**, 044122.
[32] K. Hosseini, P. Trus, A. Frenzel, C. Werner and E. Fischer-Friedrich, *Soft Matter*, 2022, **18**, 2585–2596.
[33] J. Landsgesell, P. Hebbeker, O. Rud, R. Lunkad, P. Košovan and C. Holm, *Macromolecules*, 2020, **53**, 3007–3020.
[34] A. Bakhshandeh, D. Frydel and Y. Levin, *The Journal of Chemical Physics*, 2022, **156**, 014108.
[35] C. Labbez and B. Jönsson, International Workshop on Applied Parallel Computing, 2006, pp. 66–72.
[36] W. Smith and B. Triska, *The Journal of chemical physics*, 1994, **100**, 3019–3027.
[37] J. K. Johnson, A. Z. Panagiotopoulos and K. E. Gubbins, *Molecular Physics*, 1994, **81**, 717–733.
[38] C. E. Reed and W. F. Reed, *The Journal of chemical physics*, 1992, **96**, 1609–1620.
[39] Y. Levin and A. Bakhshandeh, *Soft Matter*, 2023, **19**, 3519–3521.
[40] Y. Levin and A. Bakhshandeh, *The Journal of Chemical Physics*, 2023, **159**, 111101.
[41] A. Bakhshandeh and Y. Levin, *The Journal of Physical Chemistry B*, 2023, **127**, 9405–9411.
[42] B. R. Svensson and C. E. Woodward, *Molecular Physics*, 1988, **64**, 247–259.
[43] P. Sloth and T. S. Sørensen, *Chemical physics letters*, 1990, **173**, 51–56.
[44] R. Euwema and G. Surratt, *Journal of Physics and Chemistry of Solids*, 1975, **36**, 67–71.